EXPERIMENTAL CELL RESEARCH 318 (2012) 288–297

Available online at www.sciencedirect.com

SciVerse ScienceDirect

www.elsevier.com/locate/yexcr

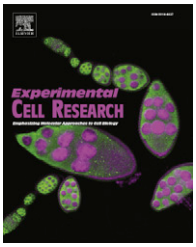

Research Article

Visualizing the effect of hypoxia on fluorescence kinetics in living HeLa cells using the fluorescent ubiquitination-based cell cycle indicator (Fucci)

*Atsushi Kaida, Masahiko Miura**

Oral Radiation Oncology, Department of Oral Restitution, Graduate School of Medical and Dental Sciences, Tokyo Medical and Dental University, 1-5-45 Yushima, Bunkyo-ku, Tokyo 113-8549, Japan

ARTICLE INFORMATION

Article Chronology:
Received 13 August 2011
Revised version received
9 October 2011
Accepted 26 October 2011
Available online 3 November 2011

Keywords:
Fluorescent protein
Monomeric Azami Green (mAG)
Monomeric Kusabira Orange 2 (mKO2)
Hypoxia
Fluorescent ubiquitination-based cell cycle indicator (Fucci)

ABSTRACT

Fluorescent proteins are widely used for the direct visualization of events such as gene expression and subcellular localization in mammalian cells. It is well established that oxygen is required for formation of functional chromophore; however, the effect of hypoxia on fluorescence emission has rarely been studied. For this purpose, under hypoxic conditions, we investigated the kinetics of red and green fluorescence in HeLa cells from two fluorescent proteins, monomeric Kusabira Orange 2 (mKO2) and monomeric Azami Green (mAG), respectively, using the fluorescent ubiquitination-based cell cycle indicator (Fucci). In this system, cells in G1 or other phases emit red or green fluorescence, respectively. We found that hypoxia abrogated both red and green fluorescence about ~10 h after the treatment, although their protein levels were almost maintained. The treatment did not significantly affect fluorescence in cells constitutively expressing the same fluorescent proteins lacking the ubiquitin ligase-binding domains. The abrogation of fluorescence resulted from a combination of ubiquitination-dependent degradation of pre-existing functional proteins during specific cell cycle phases, and the expression of newly synthesized non-fluorescent proteins containing non-oxidized chromophore during hypoxic treatment. Indeed, non-fluorescent cells after hypoxic treatment gradually developed fluorescence after reoxygenation in the presence of cycloheximide; kinetics of recovery were much faster for mAG than for mKO2. Using the Fucci system, we could clearly visualize for the first time the effect of hypoxia on the fluorescence kinetics of proteins expressed in living mammalian cells.

Introduction

The green fluorescent protein (GFP) was originally identified in the bioluminescent jellyfish *Aequorea victoria* by Shimomura et al. [1]; thereafter, many GFP-like proteins have been discovered and developed [2–5]. GFP-like proteins now play pivotal roles in the field of molecular biology and cellular biology, especially in direct visualization of cellular events including gene expression, subcellular localization, and protein interactions [3,6,7]. The molecular basis of GFP's function and chromophore formation has also been extensively studied; the most notable characteristic is that the chromophore forms intrinsically [3,8,9]. The formation of functional chromophore in GFP-like proteins involves three major steps: protein folding, cyclization of the tripeptide

* *Corresponding author.* Fax: +81 3 5803 5897.
E-mail address: masa.mdth@tmd.ac.jp (M. Miura).

0014-4827/$ – see front matter © 2011 Elsevier Inc. All rights reserved.
doi:10.1016/j.yexcr.2011.10.016

chromophore motif, and oxidation of the cyclized chromophore; these steps appear to be commonly required for the maturation of a range of chromophores [2,3]. Molecular oxygen appears to be essential for the oxidation reaction at the 3rd step, and the reaction is likely to be rate-limiting [2,8,10]. The kinetics of the oxidation process have been studied, using *Escherichia coli* or yeast cells expressing GFP and cultured under anaerobic conditions [2,9,11,12]. However, such properties have never been studied in living mammalian cells.

The fluorescent ubiquitination-based cell cycle indicator (Fucci) was developed to visualize the dynamics of cell cycle progression [13]. HeLa-Fucci cells express two fusion proteins: monomeric Kusabira Orange 2 (mKO2) fused to amino acids 30–120 of Cdt1, which includes the Cy motif, a binding site for the E3 ligase, SCF^{Skp2}; and monomeric Azami Green (mAG) fused to amino acids 1–110 of Geminin, which includes the nuclear localizing signal (NLS) and the destruction box, a binding site for the E3 ligase, APC/C^{Cdh1}. This combination of fusion proteins causes cells to emit red fluorescence at G1 phase and green fluorescence in S/G2/M phases. Cells emit no fluorescence at early G1 phase immediately after mitosis, and emit both red and green fluorescence at G1/S transition. We believe that this system will contribute greatly to the elucidation of complicated cell cycle kinetics in solid tumors, including hypoxic subpopulations, that arise following anti-cancer treatment in pre-clinical studies of cancer therapeutics. Considering that oxygen is required for the formation of a functional chromophore [2,10–12], it is conceivable that fluorescence kinetics may be influenced under low oxygen tension in living mammalian cells. Elucidation of such properties is important for accurate determination of true cell cycle kinetics based on interpretation of the fluorescence behavior of Fucci in vivo. In this study, using the Fucci model, we explored for the first time the effect of low oxygen tension on fluorescence kinetics of mAG and mKO2 expressed in HeLa-Fucci cells.

Material and methods

Cell lines and culture conditions

HeLa cells expressing the Fucci probes (HeLa-Fucci) were provided by the RIKEN BRC through the National Bio-Resource Project of the MEXT, Japan. HeLa cells were obtained from the Health Science Research Resources Bank (Sendai, Japan). Cells were maintained in DMEM (Sigma-Aldrich, St. Louis, MO) without antibiotics supplemented with 10% fetal bovine serum, at 37 °C in a 5% CO_2 humidified atmosphere.

Plasmids and transfection

A humanized monomeric Azami-Green (phmAG1-MC1) expression vector and a humanized monomeric Kusabira-Orange 2 (phmKO2-MC1) expression vector were purchased from Medical and Biological Laboratories (Nagoya, Japan). To establish HeLa cells constitutively expressing mAG or mKO2, parent cells were transfected with each plasmid using Lipofectamine LTX (Invitrogen, Carlsbad, CA) agents. Transfected cells were selected with 1.0 mg/ml Geneticin (Sigma-Aldrich, St. Louis, MO) and resultant clones were developed. Clones expressing strong fluorescence were established and designated HeLa-mAG and HeLa-mKO2.

Drug treatment and irradiation

Cells were treated with 3 mM hydroxyurea (HU) (Sigma-Aldrich, St. Louis, MO) or 20 μg/ml cycloheximide (CHX) (Sigma-Aldrich, St. Louis, MO). Cells were also irradiated at a dose of 10 Gy with an RX-650 cabinet X-radiator system (130 kVp, 5 mA, 0.5 mm Al filtration) (Faxitron, Lincolnshire, IL) at a dose rate of 0.781 Gy/min. After each treatment, fluorescence was observed or cells were prepared for Western blotting at the indicated times.

Fluorescent imaging

Fluorescent images were taken using a BIOREVO BZ-9000 fluorescence microscope (KEYENCE, Osaka, Japan). For the time-lapse imaging, cells were held in an incubation chamber at 37 °C or room temperature in a humidified atmosphere containing 5% CO_2 (Tokai Hit, Fujinomiya, Japan), except in the case of hypoxic treatment as described below. For quantitative analysis of fluorescent cells, the percentages of green, red, orange (both green and red), and non-fluorescent cells were determined by counting at least 100 cells in three independent fields.

Hypoxic treatment

When almost anoxic conditions are required in radiobiological studies, e.g., in order to determine oxygen enhancement ratio [14], glass petri dishes instead of plastic dishes have been used in conjunction with a gas mixture of 95% N_2 and 5% CO_2, in order to overcome the problem of dissolved oxygen contained in plastic dishes [15,16]. However, for other purposes, plastic dishes are commonly used [17–22]; indeed, glass petri dishes with thick bottoms are not suitable for high quality cell imaging. Therefore, in this study we established hypoxic conditions by a combination of plastic culture dishes and an AnaeroPack-Anaero 5% system (Mitsubishi Gas Chemical, Tokyo, Japan) [18,20–22], using catalysts that contain sodium ascorbate as the principal ingredient in conjunction with a carbon dioxide absorber to scavenge the carbon dioxide in a tightly closed 2.5 L jar (Mitsubishi Gas Chemical) [21]. This is a much simpler method than using the mixed gas. The oxygen tension (pO_2) in the atmosphere was monitored by putting an OXY-1 oxygen monitor (JIKCO, Tokyo, Japan) in the jar, along with the catalyst and the plastic dishes containing HeLa cells and medium. The entire experimental rig was maintained at 37 °C. The kinetics after hypoxic treatment are presented in Supplementary Fig. 1. We confirmed that this system could reproducibly and rapidly decrease the pO_2 in the atmosphere rapidly, reaching $pO_2 < 0.1\%$ within an hour, in accordance with the manufacturer's data (Mitsubishi Gas Chemical).

Cells were plated in tissue culture plastic dishes and subcultured for 24 h before hypoxic treatment. Dishes were put into a plastic jar (2.5 L) with a bag including the catalyst and the jar was closed tightly. The jar was maintained at 37 °C or room temperature for the indicated times. The CO_2 tension is maintained at 5% for at least 24 h in this condition [18,20]. For the time-lapse imaging of cells in hypoxia, the time-lapse observation protocol using the fluorescence microscope was adapted to a small-volume jar (0.5 L; Mitsubishi Gas Chemical). The incubation chamber was not used in this experiment; the pre-incubated jar containing the dish at 37 °C was transferred to the stage of the fluorescence microscope, and cells were observed at the room temperature for a short period. In all hypoxic experiments, the

Anaero-Indicator (Mitsubishi Gas Chemical) was used to confirm that the pO_2 in the atmosphere remained at <0.1%.

Flow cytometric analysis

Immediately after treatments, collected culture medium and trypsinized cells were centrifuged, and cell pellets were washed in ice-cold phosphate-buffered saline (PBS). Cells were fixed in ice-cold 70% ethanol in PBS for at least 30 min on ice. After fixation, cells were re-washed in ice-cold PBS and incubated in 0.5 μg/ml 7-AAD solution (BD Bioscience, San Jose, CA). Finally, fixed single cell suspensions were passed through a nylon mesh. Each sample was analyzed with a FACScalibur flow cytometer (Becton Dickinson, Franklin Lakes, NJ) using the FlowJo software (Tree Star, Ashland, OR).

Western blotting

Monomeric Azami-Green (mAG), monomeric Kusabira-Orange 2 (mKO2), von Hippel–Lindau protein (pVHL), and actin were detected by Western blotting. Briefly, cells were lysed with Mammalian Protein Extraction Reagent (M-PER) (Pierce, Rockford, IL) and equal amounts of cell lysate were separated using SDS-PAGE. The proteins were transferred to nitrocellulose membranes, and the membranes were blocked in 2% ECL advance blocking agent (GE Healthcare, Uppsala, Sweden) in Tris-buffered saline with Triton X-100. Proteins were detected with specific primary antibodies for mAG, mKO2 (Medical and Biological Laboratories, Nagoya, Japan), pVHL (clone Ig32; BD Pharmingen, San Diego, CA), and actin (clone C4; Millipore, Billerica, MA). Specific proteins were visualized by using secondary antibodies conjugated with horseradish peroxidase (Santa Cruz Biotechnology, Santa Cruz, CA) and the ECL Western Blotting Detection reagents (GE Healthcare). Protein expression levels were quantified using the Image J 1.44 software (available from a website at http://rsbweb.nih.gov/ij/) and expressed as normalized by actin expression levels.

Kinetic analysis of fluorescence recovery after reoxygenation

Immediately after the hypoxic treatment for 16 h, cells were treated with CHX (20 μg/ml) and held in an incubation chamber at 37 °C in a humidified atmosphere containing 5% CO_2, and visualized by time-lapse microscope. For fluorescence intensity analysis, images were taken every 4 min or 20 min intervals. Four cells showing green or red fluorescence after recovery were selected, and fluorescence intensity within each nucleus was quantified using the Dynamic Cell Count software (KEYENCE, Osaka, Japan). Green and red fluorescence signals were robustly detectable 4 min and 40 min after admission of air, respectively. The fluorescence intensity was plotted against time; curves were then normalized by simple subtraction so that the initial measurable points start at zero, and fluorescence intensity was re-plotted against time t. These curves were fitted to the following equation using the KaleidaGraph 3.6 (Synergy Software, Reading, PA):

$$F = s\{1-\exp(-kt)\}$$

where F represents fluorescence intensity at time t, s represents saturated intensity of fluorescence at $t=\infty$, and k represents the rate constant. Time constant τ was also determined using the equation $\tau = (\ln 2)/k$.

Statistical analysis

Mean values were statistically compared using the two-tailed t-test. p Values <0.05 were considered statistically significant.

Results

Fluorescence from HeLa-Fucci cells is abrogated under hypoxic conditions

Using HeLa-Fucci cells, we previously reported that X-irradiation gradually increased the number of cells emitting green fluorescence, reaching a peak about 16 h after irradiation; thereafter, the number decreased again. The kinetics corresponded closely to the accumulation and release kinetics of G2/M phase cells [23,24]. In the present study, we confirmed that the kinetics of the fluorescence were consistent not only with the cell cycle change, but also with protein expression levels of mAG and mKO2 (Figs. 1A–E). A similar relationship among fluorescence, cell cycle change, and protein expression levels was also observed after hydroxyurea (HU) treatment. However, HU induces arrest in or near early S phase [25–27] (Figs. 1F–J); therefore, HU-arrested cells should emit only green fluorescence following the G1/S transition, confirming our previous study [24]. Thus the kinetics of Fucci fluorescence correlated well with those of cell cycle distribution and protein expression levels following these treatments.

When cells were incubated in hypoxic conditions, the results were quite different. The number of cells emitting either red or green fluorescence decreased gradually, and almost no cells emitted fluorescence up to 10–16 h after the onset of hypoxic treatment (Fig. 1K). The fluorescence signals never returned thereafter up to 40 h (Fig. 1K). In the Fucci system, there is a short period at early G1 phase immediately after the end of mitosis during which cells exhibit no fluorescence or no reporter protein expression [13]. However, 6 and 16 h after the onset of hypoxic treatment both mAG and mKO2 protein levels were comparable to those in control cells albeit with a slight decrease (Figs. 1O and P); therefore, it was unlikely that cells were completely arrested at early G1 phase. The level of mKO2 protein gradually decreased after the complete disappearance of fluorescence, and became undetectable about 40 h after the treatment (Figs. 1K,M, and O). Judging from fluorescent protein expression and DNA content, it is likely that partial G1 arrest first occurs ~16 h after hypoxic treatment; subsequently, cells accumulate slowly in early S-phase during hypoxic treatment (Figs. 1L,N,O, and P). These cell cycle events occur after both red and green fluorescence signals are almost abrogated. In this hypoxic condition, cell viability remained high even 40 h after treatment; dead cells floating in medium were observed only rarely and viability as determined by Trypan blue exclusion test was 95%. Therefore, we tentatively concluded that the fluorescence kinetics observed during the hypoxic treatment might be independent of cell cycle progression.

Fluorescence from cells constitutively expressing mAG and mKO2 is retained under hypoxic conditions

It may be possible that hypoxia directly affects the function of the chromophores of fluorescent proteins, because oxygen is an essential factor in the formation of functional chromophores [2,8]. To

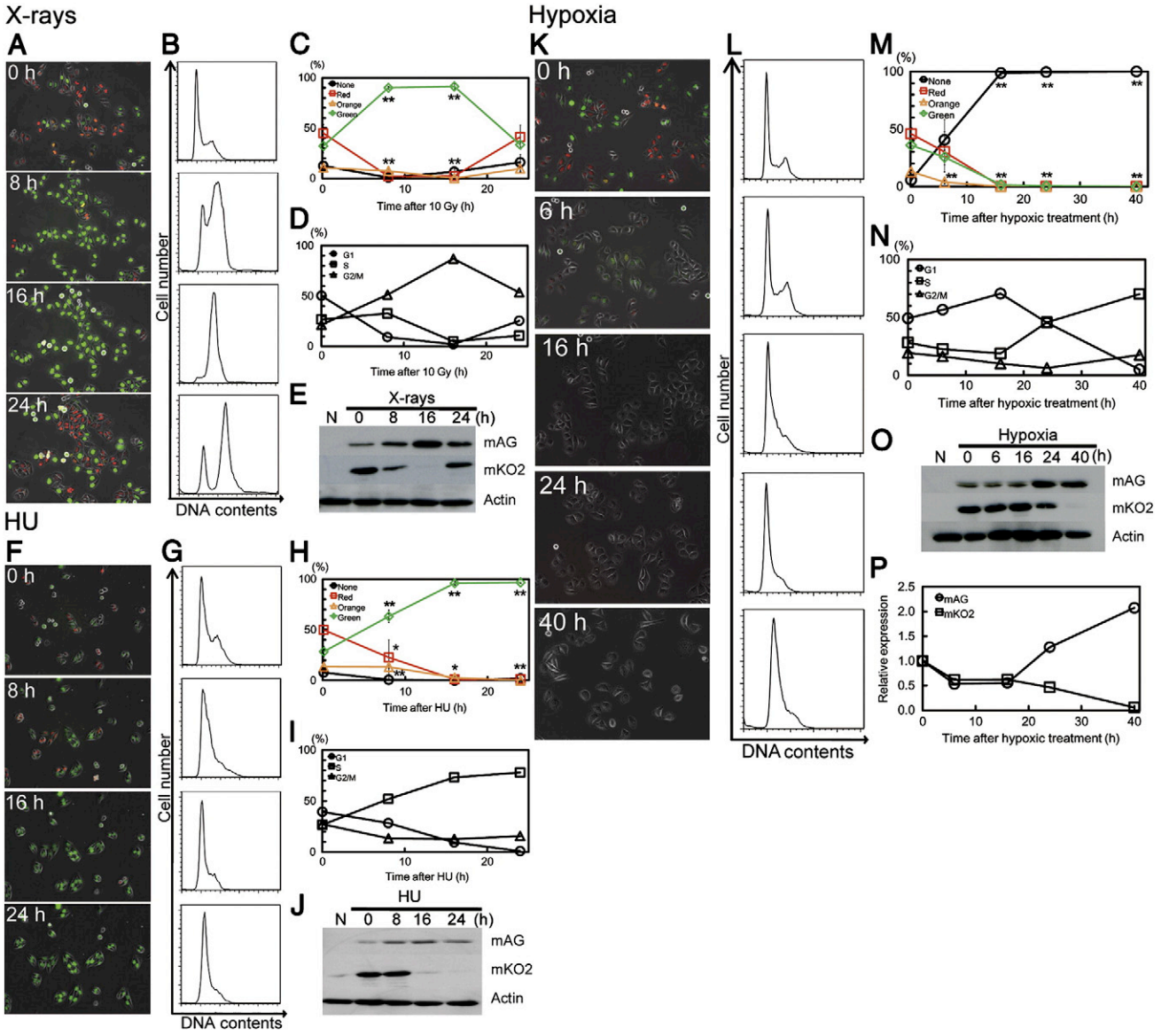

Fig. 1 – Kinetics of fluorescence, DNA content, and protein expression of mAG and mKO2 in HeLa-Fucci cells after treatment with irradiation, HU, or hypoxia. A, F, and K: Fluorescent images after each treatment at the indicated times. A and F were generated by time-lapse imaging. B, G, and L: Histograms of DNA content obtained by flow cytometric analysis after each treatment at the indicated times. C, H, and M: Percentages of green, red, orange (both green and red), and non-fluorescent cells after each treatment at the indicated times. Data are expressed as means ± SD in three different fields. C: $^{**}p < 0.01$ vs. untreated cells. None: 8 h; Red and Green: 8 and 16 h; Orange: 16 h. H: $^{**}p < 0.01$ vs. untreated cells. None: 8 and 16 h; Red: 24 h; Orange: 24 h; Green: 8, 16, and 24 h. H: $^{*}p < 0.05$ vs. untreated cells. Red: 8 and 16 h. M: $^{**}p < 0.01$ vs. untreated cells. None, Red, and Green: 16, 24, and 40 h. Orange: 8, 16, 24, and 40 h. D, I, and N: Percentages of cells in G1, S, and G2/M after each treatment at the indicated times. E, J, and O: Protein expression of mAG and mKO2 measured by Western blotting after each treatment at the indicated times. N, Negative control from parental HeLa cells. P: Relative expression of mAG and mKO2 proteins, normalized against actin expression in Fig. 1O. Data shown here are representatives of 2–3 independent experiments.

test this possibility, we transfected HeLa cells with plasmids encoding cDNA for mAG or mKO2 lacking degradation signals, i.e. 'degrons' (Fig. 2A), and established clones expressing high levels of mAG or mKO2 proteins (Fig. 2B). Time-lapse imaging revealed that these cells constitutively emitted the appropriate fluorescent signals irrespective of cell cycle phase (Fig. 2C). Interestingly, in remarkable contrast to HeLa-Fucci cells, the fluorescent signals from cells expressing proteins that lacked the degrons were not significantly affected during the hypoxic treatment even 30 h after the onset of hypoxic treatment (Figs. 2D and E). These results unequivocally demonstrate that hypoxia does not directly affect the function of the chromophores in either mAG or mKO2.

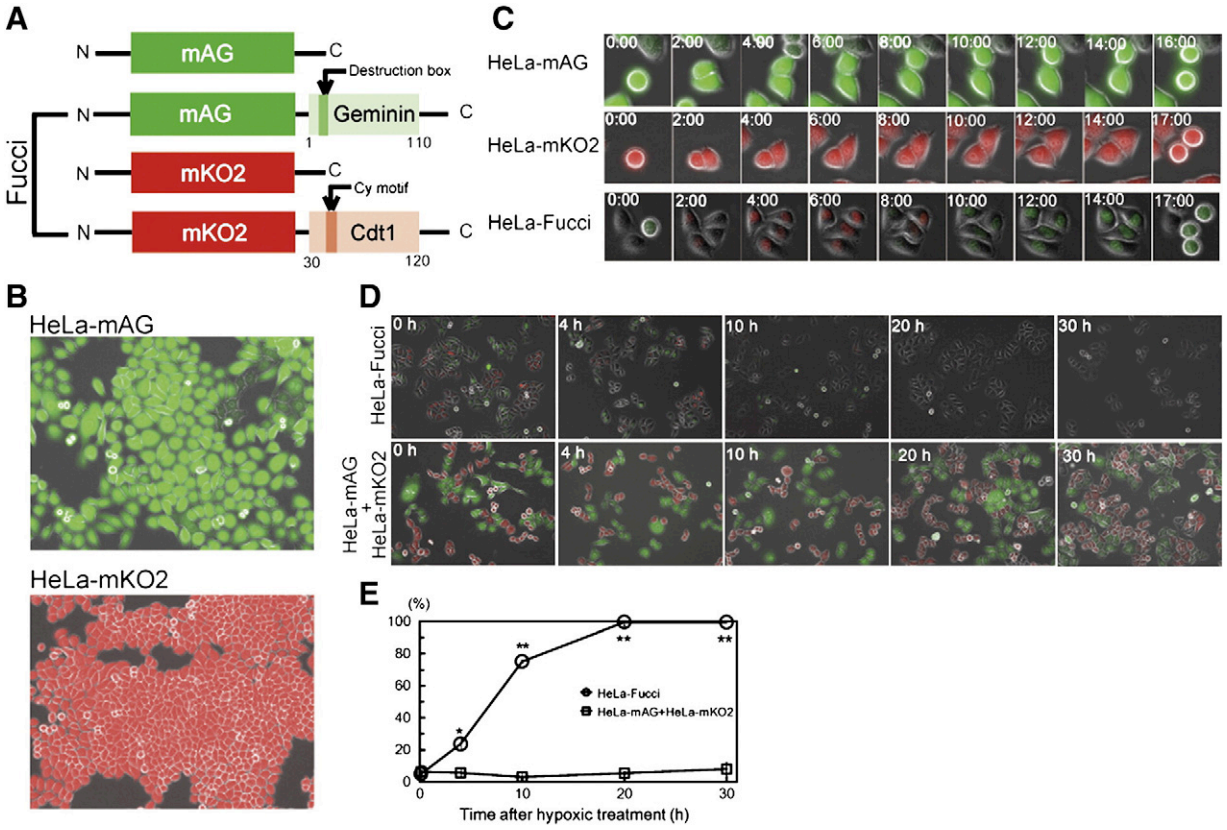

Fig. 2 – Characterization of HeLa cells constitutively expressing mAG or mKO2 lacking the degrons. A, Comparison of protein structures among the Fucci probes and singly expressed, non-degradable mAG or mKO2. B, Fluorescent images of HeLa-mAG and HeLa-mKO2 cells. C, Time-lapse imaging of fluorescence during one cell cycle period in HeLa-mAG, HeLa-mKO2, and HeLa-Fucci cells. Time is shown as hours:minutes with a starting point at 00:00. D, Kinetics of fluorescence in HeLa-Fucci cells, and mixed cultures of HeLa-mAG cells and HeLa-mKO2 cells, under hypoxic conditions. E, Percentages of non-fluorescent cells in HeLa-Fucci cells, and mixed cultures of HeLa-mAG cells and HeLa-mKO2 cells, under hypoxic conditions. Data are expressed as means ± SD in three different fields. In most cases, SD bars are smaller than symbols. $^{**}p < 0.01$ vs. untreated cells. HeLa-Fucci cells: 10 h, 20, and 30 h. $^{*}p < 0.05$ vs. untreated cells. HeLa-Fucci cells: 4 h. Data shown here are representatives of at least three experiments.

Cell cycle progression is required for abrogation of fluorescence from HeLa-Fucci cells under hypoxic conditions

HeLa-Fucci cells were treated with cycloheximide (CHX) to examine the stability of fluorescent proteins; however, we noticed that this treatment halted the cell cycle progression, as shown by the finding that the indicative fluorescence color change was not detected (Fig. 3C). Indeed, this function of CHX has already been reported by other investigators [28,29]. Under this condition, these proteins were likely to be quite stable. It is well-known that incubation at room temperature (RT) stops cell cycle progression [30,31]. The change of fluorescence in HeLa-Fucci cells was clearly detected up to ~24 h after the RT treatment; thereafter, the change was not significantly detected (Fig. 3E). Taking advantage of these properties, we examined the effect of cell cycle progression on fluorescence kinetics under hypoxic conditions. In contrast to control cells receiving only hypoxic treatment (Fig. 3B), neither CHX (Fig. 3D) nor RT treatment (Fig. 3F) significantly reduced the number of cells emitting the fluorescence under hypoxic conditions. Furthermore, HU-treated cells arrested at around early S phase did not exhibit a significant reduction of green fluorescence under hypoxic conditions (Fig. 3H). Quantitative analysis of non-fluorescent cells after hypoxic treatment, combined with each treatment described above, is presented in Supplementary Fig. 2. These results indicate that cell cycle progression is required for the abrogation of fluorescence under hypoxic conditions.

Fluorescence signals disappear at specific cell cycle phases, but the subsequent signals do not appear under hypoxic conditions

In the Fucci system, both fluorescent proteins are constitutively generated; protein levels are regulated by ubiquitination-based degradation [13]. Furthermore, only mAG and mKO2 with E3 ligase-binding domains exhibited abrogation of the fluorescence under hypoxic conditions (Fig. 2). It is thus reasonable that degradation according to the principle of the Fucci could be the main mechanism underlying fluorescence abrogation under hypoxic conditions; this idea is consistent with the fact that cell cycle progression is required for the abrogation of fluorescence (Fig. 3).

To confirm this, we set up time-lapse imaging observation for HeLa-Fucci cells under hypoxic conditions. Although we used a 2.5 L jar to create hypoxic conditions for our previous observations, in the time-lapse observations we tested a jar of smaller

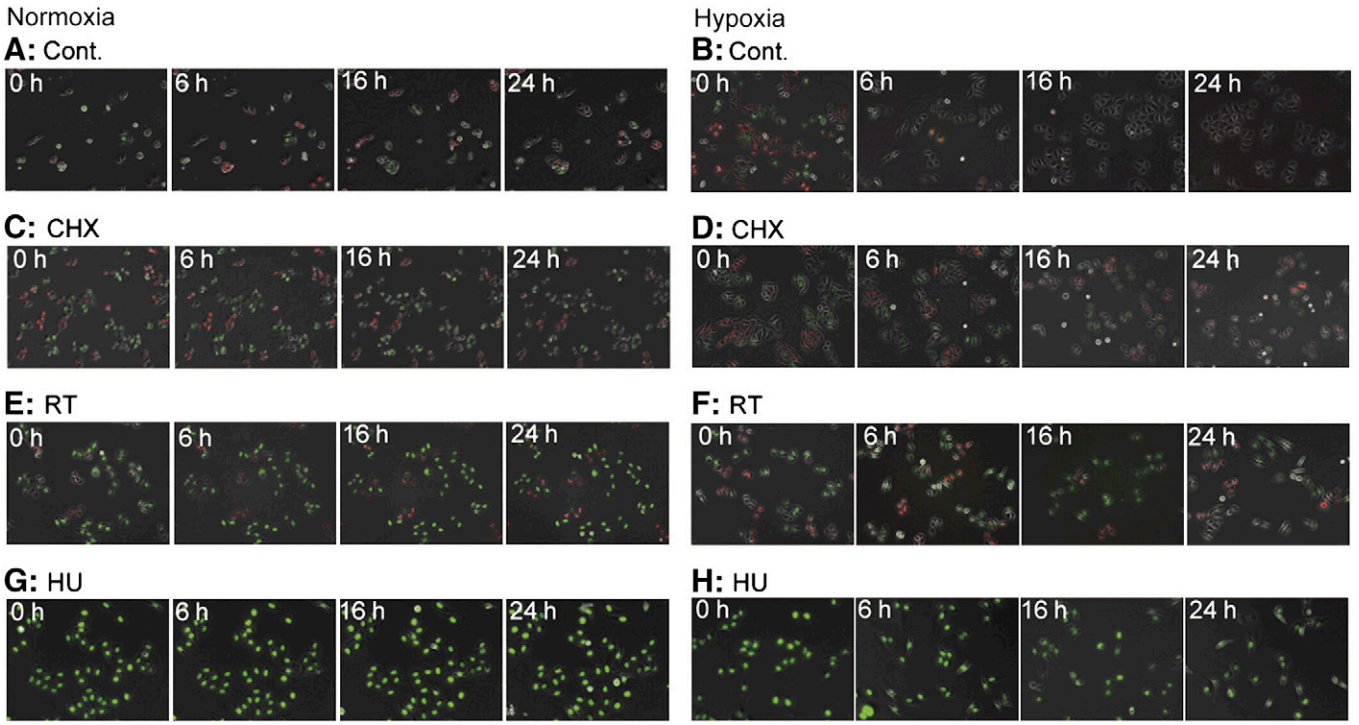

Fig. 3 – Effect of cell cycle inhibition on fluorescence emission in HeLa-Fucci cells under hypoxic conditions. A and B: Control. C and D: CHX treatment. Cells were treated with 20 μg/ml CHX for 2 h, and observation started in the presence of CHX (= 0 h). Hypoxic treatment also started 2 h after the CHX treatment. E and F: Room temperature treatment (RT). Cells were treated at room temperature for 24 h and then observation was started at 0 h. Hypoxic treatment was started 24 h after RT treatment in normoxia. G and H: hydroxyurea (HU) treatment. Cells were treated with 3 mM HU for 24 h, and then observation started in the presence of HU (= 0 h). Hypoxic treatment was started 24 h after the HU treatment. A, C, E, and G: Time-lapse images; B, D, F, and H: Images of different fields in different dishes. A representative experiment of two to three performed is shown.

volume (0.5 L) to adapt the system. Under this condition, it was not possible to control temperature. The jar and dish were pre-heated at 37 °C and then transferred to the stage of the fluorescence microscope, and cells were observed for a relatively short period (~6 h) albeit with a low imaging quality. During that time, almost normal cell cycle progression was observed. In normoxia, transition from M to G1 phase was accompanied by the fluorescence shift from green to red after a short non-fluorescence phase (Fig. 4A, upper panels); however, in hypoxia, red did not appear after disappearance of green (Fig. 4A, lower panels). Similarly, in normoxia, transition from G1 to S phase was accompanied by a fluorescence shift from orange (both emission of red and green) to green due to the degradation of mKO2 at this phase (Fig. 4B, upper panels). In hypoxia, cells already fluorescing orange exhibited exactly the same pattern as that observed in normoxia (data not shown). However, cells fluorescing red gradually disappeared without passing through an orange stage; consequently, green never appeared (Fig. 4B, lower panels). These findings strongly support the notion that the disappearance of fluorescence in both mAG and mKO2 after hypoxic treatment depends on the Fucci mechanism: mAG is degraded by the activity of APC/C^{cdh1} at the end of mitosis, and that mKO2 is degraded by SCF^{skp2} at G1/S phase. Furthermore, the subsequent fluorescence signals turned out not to emerge after disappearance of the signals under hypoxic conditions.

Recovery of fluorescence in non-functional proteins after reoxygenation

Fig. 1 showed that when fluorescence was completely lost, fluorescent protein levels at the time were comparable to those in control samples, indicating that newly synthesized proteins should be produced normally during hypoxic treatment. Because molecular oxygen is required for functional chromophore formation, newly synthesized proteins may be non-fluorescent, which is suggested by the findings in Fig. 4. If this is the case, such initially non-functional proteins should be able to fully develop fluorescence after reoxygenation in the presence of CHX. For this purpose, time-lapse imaging was performed after admission of air, in order to detect the recovery of fluorescence after hypoxic treatment. We found that green fluorescence recovered quickly, while red fluorescence was recovered more slowly after a ~30 min lag period (Fig. 5). Kinetic analysis using normalized data revealed that recovery of both fluorescent signals followed a simple exponential approach to the final steady state (Supplementary Fig. 3). This result strongly implies that anaerobically synthesized chromophores have already cyclized, and is competent to form a functional chromophore once oxygen is provided. We conclude that newly synthesized proteins during the hypoxic treatment are present in their non-oxidized, non-fluorescent intermediate forms. The time constants assuming pseudo-first order kinetics were approximately 7 times higher for mKO2 than for mAG (Supplementary Table 1).

Discussion

In this study, we demonstrated several novel findings regarding the effects of low oxygen tension as shown in Supplementary Fig. 1 on fluorescence kinetics in living HeLa-Fucci cells: 1) the number of cells emitting fluorescence gradually decreased, and fluorescence was no longer detected ~10 h after the hypoxic treatment; 2) the fluorescence-emitting activity of already-synthesized, fluorescent mAG and mKO2 was not directly affected in hypoxia;

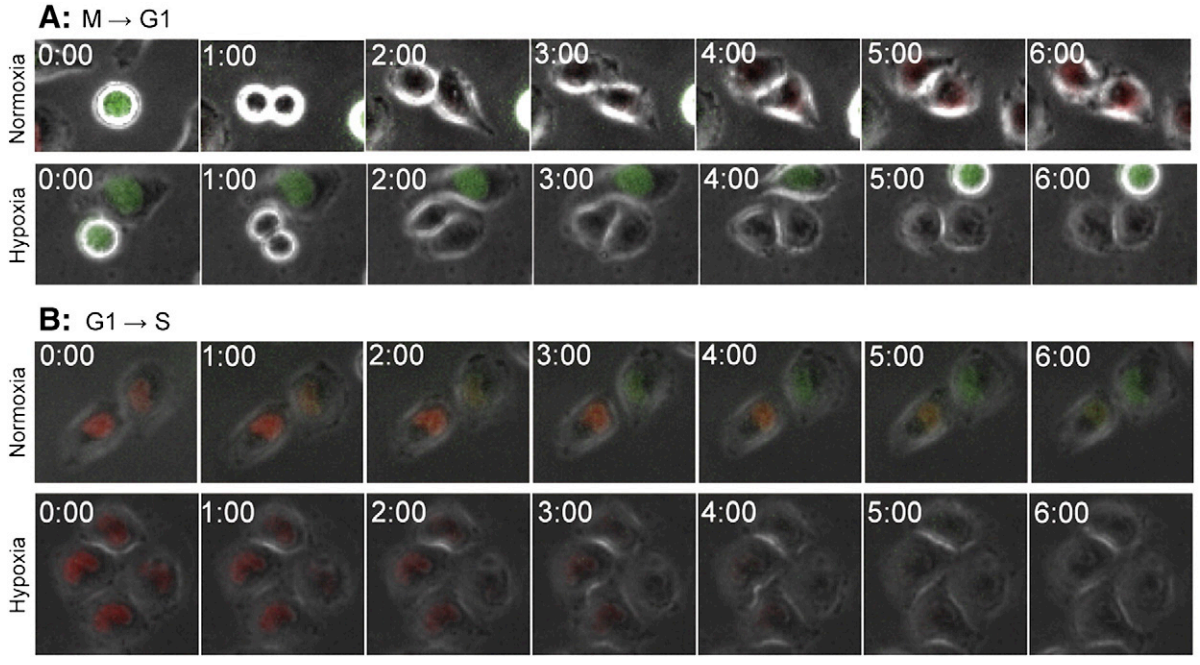

Fig. 4 – Time-lapse imaging of HeLa-Fucci cells during hypoxic treatment. A, Time-lapse imaging for HeLa-Fucci cells at the transition from M to G1 phase under normoxia or hypoxia. B, Time-lapse imaging for HeLa-Fucci cells at the transition from G1 to S phase under normoxia or hypoxia. Cells were treated with AnaeroPack in a small volume jar to adapt the method for the time-lapse imaging at RT. Time is shown as hours:minutes during a 6 h period of consecutive imaging. Representatives of multiple experiments are shown here.

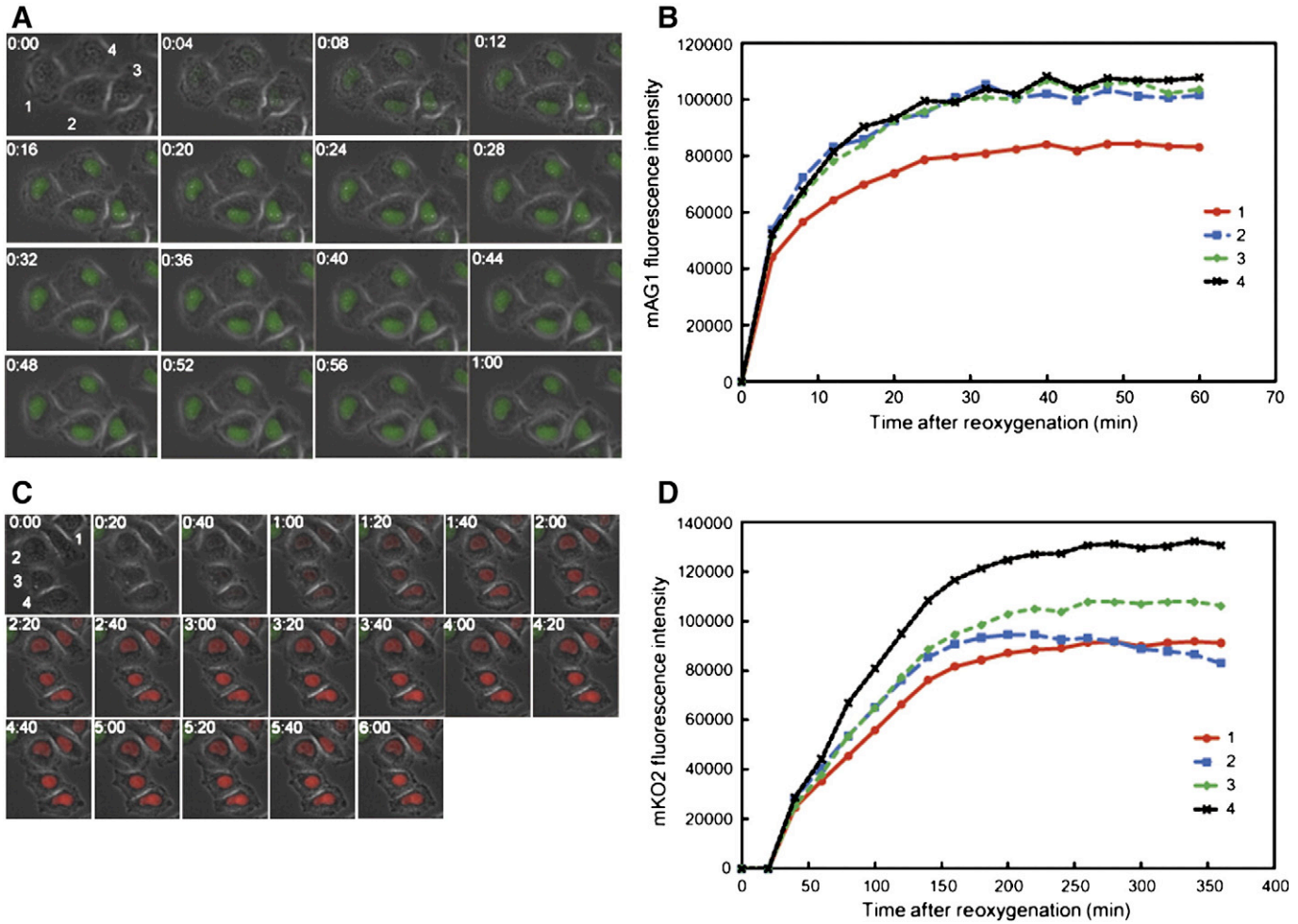

Fig. 5 – Recovery of fluorescence in hypoxia-treated HeLa-Fucci cells after admission of air. A, Time-lapse imaging of fluorescence recovery of mAG. Time is shown as hours:minutes with a starting point at 00:00.; B, Quantification of fluorescence intensity from mAG in 4 selected nuclei as a function of time. C, Time-lapse imaging of fluorescence recovery of mKO2. D, Quantification of fluorescence intensity from mKO2 in 4 selected nuclei as a function of time. Time-lapse imaging of hypoxia-treated (16 h) non-fluorescent cells started in the presence of 20 μg/ml CHX immediately after admission of air. The data shown are representative of three experiments.

3) the abrogation of fluorescence resulted from a combination of the degradation of already-synthesized mAG and mKO2, depending on the principle of Fucci, and generation of non-oxidized proteins, which do not contribute to fluorescence emission; 4) the recovery kinetics of the fluorescence after reoxygenation in the presence of CHX exhibited pseudo-first order kinetics, confirming the accumulation of non-oxidized intermediates; and 5) the time constants for the oxidation of fluorescent proteins were approximately 7 times higher in mKO2 than in mAG. The kinetics of fluorescence disappearance thus reflected that of degradation of functional proteins that were synthesized before hypoxic treatment.

We combined plastic dishes and the AnaeroPack-Anaero 5% system, which reproducibly brought the oxygen tension (pO_2) to <0.1% in the atmosphere within an hour, in order to create hypoxic conditions and retain high quality cell imaging. We could not determine the kinetics of pO_2 in the medium; however, it is a strong prediction that the pO_2 in the medium should reproducibly decrease and reach the same level as in the gas above, though at a slower rate than in the atmosphere. In this condition, cell cycle progression and high cell viability could be maintained for a significant interval thereafter. These conditions allowed us to clarify for the first time the effects of low oxygen tension on fluorescence emission from proteins expressed in mammalian cells.

Liu et al. recently reported that the expression of von Hippel–Lindau tumor-suppressor protein (pVHL) is decreased as rapidly as 4 h after hypoxic treatment, and is a novel substrate of APC/C^{Cdh1} [32]. The authors could partly explain the mechanism as a function of the APC/C^{Cdh1} activity in G1-arrested cells after hypoxic treatment. However, that was insufficient to explain the speed of degradation; apparent G1 arrest occurs around 16 h after hypoxic treatment. Therefore, the authors proposed a mechanism of degradation of pVHL also by other E3 ligases activated after a shift to hypoxia [32]. Indeed, we could confirm that pVHL was completely degraded as rapidly as 6 h after a shift to hypoxia, and was not detected up to 40 h in our hypoxia system (Supplementary Fig. 4A and B). We considered the possibility that a secondary factor might be involved in the disappearance of mAG fluorescence, because the kinetics were very similar (Figs. 1K and M); however, the mAG probe is refractory to the ligase activity and seems not to be its substrate, as shown in Supplementary Fig. 4. Even if the mAG probe is a substrate, simple degradation of proteins in a cell cycle-independent manner cannot by itself fully explain the findings. Thus, the possible involvement of the secondary factor could be ruled out. To the best of our knowledge, the mAG probe is not degraded by factors other than APC/C^{Cdh1}. So far, only the combined events, degradation of the limited quantities of mature fluorescent probes according to the Fucci principle and synthesis of non-oxidized immature probes, can explain all phenomena occurring after hypoxic treatment.

Azami Green (AG) was cloned from the *Galaxeidae* coral by Miyawaki and his colleagues [4]; the identity between AG and enhanced GFP (EGFP) at the amino acid level is only 5.7%, despite the fact that the proteins share a similar spectral profile. AG initially forms a tight tetrameric complex, which results in poor labeling of subcellular structures. Therefore, to increase its utility in visualizing subcellular events, AG was adapted to a monomeric form (mAG) by the introduction of three amino acid substitutions. Compared to EGFP, mAG has a brighter fluorescence and a more rapid maturation speed under normoxic conditions [4]. Kusabira Orange (KO) was cloned from *Fungia concinna* coral also by Miyawaki and his colleagues, and similarly adapted to the monomeric form [5]. In the development of Fucci, a fast folding variant mKO2 and mAG were used to visualize the dynamics of cell cycle progression [13]. Three dimensional analysis of the crystal structure of mKO revealed a novel three-ring chromophore developed autocatalytically from the Cys-Tyr-Glu tripeptide that constitutes the chromophore; the maturation process involves complicated oxidization steps [33]. The slow kinetics of oxidation for mKO2 obtained in this study can be attributed to its complex oxidation process. Heim et al. [10] reported that in *Escherichia coli* expressing GFP under hypoxic conditions, the time constant for oxidation of GFP was ~120 min; Siemering et al. [11] reported that the time constant was ~10 min in yeast cells expressing GFP under hypoxic conditions. Although the primary structure of mAG is quite different from that of GFP [4], the time constant for mAG expressed in HeLa-Fucci cells was ~7 min, close to that of GFP expressed in yeast cells. In mammalian cells, the oxidation process in mAG may not be rate limiting for chromophore maturation, as Siemering et al. implied in the case of yeast cells [11]. Further study will be required in order to elucidate the detailed oxidation mechanism and explain the slower kinetics observed for mKO2 in mammalian cells.

Hypoxic fractions in solid tumors experience varying levels of oxygen tension, depending on the distance from tumor vessels [34,35]; this is referred to as chronic hypoxia. Furthermore, oxygen tension periodically fluctuates due to a periodical closure and reopening of tumor vessels [35,36]; this is known as acute or cycling hypoxia. When Fucci is eventually used to analyze cell cycle kinetics of hypoxic fractions in solid tumors that experience such complicated oxygen kinetics, fluorescence kinetics may be influenced independent of cell cycle; therefore, care should be taken when interpreting the true cell cycle from the fluorescence behavior in vivo.

In conclusion, we visualized the effects of hypoxia on fluorescence kinetics in living mammalian cells using the Fucci system, which could differentiate between already-synthesized functional fluorescent proteins present before hypoxic treatment from newly synthesized non-fluorescent proteins present after hypoxic treatment. Furthermore, the kinetics of oxidization were quite different depending on the type of fluorescent protein. These properties of fluorescent proteins under hypoxic conditions should be considered when they are applied to hypoxic situations, according to the purpose of the study.

Supplementary data associated with this article can be found, in the online version, at doi:10.1016/j.yexcr.2011.10.016.

Acknowledgment

We thank Drs. A. Miyawaki and A. Sakaue-Sawano for providing the HeLa cells expressing the Fucci probes and critical reading of the manuscript. This study was supported in part by the Program for Promotion of Fundamental Studies of Health Sciences of the National Institute of Biomedical Innovation (NIBIO).

REFERENCES

[1] O. Shimomura, F.H. Johnson, Y. Saiga, Extraction, purification and properties of aequorin, a bioluminescent protein from the luminous hydromedusan, *Aequorea*, J. Cell. Comp. Physiol. 59 (1962) 223–239.

[2] R. Heim, D.C. Prasher, R.Y. Tsien, Wavelength mutations and posttranslational autoxidation of green fluorescent protein, Proc. Natl. Acad. Sci. U. S. A. 91 (1994) 12501–12504.
[3] R.Y. Tsien, The green fluorescent protein, Annu. Rev. Biochem. 67 (1998) 509–544.
[4] S. Karasawa, T. Araki, M. Yamamoto-Hino, A. Miyawaki, A green-emitting fluorescent protein from *Galaxeidae* coral and its monomeric version for use in fluorescent labeling, J. Biol. Chem. 278 (2003) 34167–34171.
[5] S. Karasawa, T. Araki, T. Nagai, H. Mizuno, A. Miyawaki, Cyan-emitting and orange-emitting fluorescent proteins as a donor/acceptor pair for fluorescence resonance energy transfer, Biochem. J. 381 (2004) 307–312.
[6] D.A. Zacharias, R.Y. Tsien, Molecular biology and mutation of green fluorescent protein, Methods Biochem. Anal. 47 (2006) 83–120.
[7] B.N. Giepmans, S.R. Adams, M.H. Ellisman, R.Y. Tsien, The fluorescent toolbox for assessing protein location and function, Science 312 (2006) 217–224.
[8] A.B. Cubitt, R. Heim, S.R. Adams, A.E. Boyd, L.A. Gross, R.Y. Tsien, Understanding, improving and using green fluorescent protein, Trends Biochem. Sci. 20 (1995) 448–455 (1995).
[9] M. Ormo, A.B. Cubitt, K. Kallio, L.A. Gross, R.Y. Tsien, S.J. Remingston, Crystal structure of the *Aequorea victoria* green fluorescent protein, Science 272 (1996) 1392–1395.
[10] R. Heim, A.B. Cubitt, R.Y. Tsien, Improved green fluorescence, Nature 373 (1995) 663–664.
[11] K.R. Siemering, R. Golbik, R. Sever, J. Haseloff, Mutations that suppress the thermosensitivity of green fluorescent protein, Curr. Biol. 6 (1996) 1653–1663.
[12] B.G. Reid, G.C. Flynn, Chromophore formation in green fluorescent protein, Biochemistry 36 (1997) 6786–6791.
[13] A. Sakaue-Sawano, H. Kurosawa, T. Morimura, A. Hanyu, H. Hama, H. Osawa, S. Kashiwagi, K. Fukami, T. Miyata, H. Miyoshi, T. Imamura, M. Ogawa, H. Masai, A. Miyawaki, Visualizing spatiotemporal dynamics of multicellular cell-cycle progression, Cell 132 (2008) 487–498.
[14] E.J. Hall, J. Giaccia, Repair of radiation damage and the dose rate effect, in: E.J. Hall, J. Giaccia (Eds.), Radiobiology for the Radiologist, 6th ed., Lippincott Williams & Wilkins, Philadelphia, 2009, pp. 85–105.
[15] J.D. Chapman, J. Sturrock, J.W. Boag, J.O. Crookall, Factors affecting the oxygen tension around cells growing in plastic petri dishes, Int. J. Radiat. Biol. 17 (1979) 305–328.
[16] N. Chan, M. Koritzinsky, H. Zhao, R. Bindra, P.M. Glazer, S. Powell, A. Belmaaza, B. Wouters, R.G. Bristow, Chronic hypoxia decreases synthesis of homologous recombination proteins to offset chemoresistance and radioresistance, Cancer Res. 68 (2008) 605–614.
[17] H. Harada, S. Itasaka, S. Kizaka-Kondoh, K. Shibuya, K. Shinomiya, M. Hiraoka, The Akt/mTOR pathway assures the synthesis of HIF-1alpha protein in a glucose- and reoxygenation-dependent manner in irradiated tumors, J. Biol. Chem. 284 (2008) 5332–5342.
[18] K. Matsumoto, T. Arao, K. Tanaka, H. Kaneda, K. Kudo, Y. Fujita, D. Tamura, K. Aomatsu, T. Tamura, Y. Yamada, N. Saijo, K. Nishio, mTOR signal and hypoxia-inducible factor-1 alpha regulate CD133 expression in cancer cells, Cancer Res. 69 (2009) 7160–7164.
[19] H. Okuyama, H. Endo, T. Akashika, K. Kikuya, M. Inoue, Downregulation of c-MYC protein levels contributes to cancer cell survival under dual deficiency of oxygen and glucose, Cancer Res. 70 (2010) 10213–10223.
[20] C. Katoh, T. Osanai, H. Tomita, K. Okumura, Brain natriuretic peptide is released from human astrocytoma cell line U373MG under hypoxia: a possible role in anti-apoptosis, J. Endocrinol. 208 (2011) 51–57.
[21] T. Kamiya, A.H. Kwon, T. Kanemaki, Y. Matsui, S. Uetsuji, T. Okumura, Y. Kamiyama, A simplified model of hypoxic injury in primary cultured rat hepatocytes, In Vitro Cell. Dev. Biol. Anim. 34 (1998) 131–137.
[22] Y. Sato, H. Endo, H. Okuyama, T. Takeda, H. Iwahashi, A. Imagawa, K. Yamagata, I. Shimomura, M. Inoue, Cellular hypoxia of pancreatic β-cells due to high levels of oxygen consumption for insulin secretion in vitro, J. Biol. Chem. 286 (2011) 12524–12532.
[23] M. Ishikawa, Y. Ogihara, M. Miura, Visualization of radiation-induced cell cycle-associated events in tumor cells expressing the fusion protein of Azami Green and the destruction box of human Geminin, Biochem. Biophys. Res. Commun. 389 (2009) 426–430.
[24] A. Kaida, N. Sawai, K. Sakaguchi, M. Miura, Fluorescence kinetics in HeLa cells after treatment with cell cycle arrest inducers visualized with Fucci (fluorescent ubiquitination-based cell cycle indicator), Cell Biol. Int. 35 (2011) 359–363.
[25] R.A. Tobey, N. Oishi, H.A. Crissman, Cell cycle synchronization: reversible induction of G2 synchrony in cultured rodent and human diploid fibroblasts, Proc. Natl. Acad. Sci. U. S. A. 87 (1990) 5104–5108.
[26] H. Nishitani, S. Taraviras, Z. Lygerou, T. Nishimoto, The human licensing factor for DNA replication Cdt1 accumulates in G1 and is destabilized after initiation of S-phase, J. Biol. Chem. 276 (2001) 44905–44911.
[27] A. Kurose, T. Tanaka, X. Huang, F. Traganos, W. Dai, Z. Darzynkiewicz, Effects of hydroxyurea and aphidicolin on phosphorylation of ataxia telangiectasia mutated on Ser 1981 and histone H2AX on Ser 139 in relation to cell cycle phase and induction of apoptosis, Cytometry A 69 (2006) 212–221.
[28] X. Liu, J.M. Yang, S.S. Zhang, X.Y. Liu, D.X. Liu, Induction of cell cycle arrest at G1 and S phases and camp-dependent differentiation in C6 glioma by low concentration of cycloheximide, BMC Cancer 10 (2010) 684.
[29] L. Zhang, A. Wali, C.V. Ramana, A.K. Rish, Cell growth inhibition by okadaic acid involves gut-enriched Kruppel-like factor mediated enhanced expression of c-Myc, Cancer Res. 67 (2007) 10198–10206.
[30] M.M. Elkind, H. Sutton-Gilbert, W.B. Moses, T. Alescio, R.B. Swain, Radiation response of mammalian cells in culture: V. Temperature dependence of the repair of X-ray damage in surviving cells, Radiat. Res. 25 (1965) 359–376.
[31] E.J. Hall, J. Giaccia, Repair of radiation damage and the dose rate effect, in: E.J. Hall, J. Giaccia (Eds.), Radiobiology for the Radiologist, 6th ed., Lippincott Williams & Wilkins, Philadelphia, 2009, pp. 60–84.
[32] W. Liu, H. Xin, D.T. Eckert, J.A. Brown, J.R. Gnarra, Hypoxia and cell cycle regulation of the von Hippel–Lindau tumor suppressor, Oncogene 30 (2011) 21–31.
[33] A. Kikuchi, E. Fukumura, S. Karasawa, H. Mizuno, A. Miyawaki, S. Yoshitsugu, Structural characterization of a thiazoline-containing chromophore in an orange fluorescent protein, monomeric Kusabira Orange, Biochemistry 47 (2008) 11573–11580.
[34] R.H. Thomlinson, L.H. Gray, The histological structure of some human lung cancers and the possible implications for radiotherapy, Br. J. Cancer 9 (1955) 539–549.
[35] H. Yasui, S. Matsumoto, N. Devasahayam, J.P. Munasinghe, R. Choudhuri, S. Subramanian, J.B. Mitchell, M.C. Krishna, Low-field magnetic resonance imaging to visualize chronic and cycling hypoxia in tumor-bearing mice, Cancer Res. 70 (2010) 6427–6436.
[36] S. Matsumoto, H. Yasui, J.B. Mitchell, M.C. Krishna, Imaging cycling tumor hypoxia, Cancer Res. 70 (2010) 10019–10023.